Adhesion Control of Interface between Cellulose and Polypropylene by Vapor-Phase Assisted Surface Copolymerization

doi: info:doi/10.1002/app.45647

Adhesion Control of Interface between Cellulose and Polypropylene by Vapor-Phase Assisted Surface Copolymerization

Satoshi Gomi, Haruo Nishida

Graduate School of Life Science and Systems Engineering, Kyushu Institute of Technology, 2-4 Hibikino, Wakamatsu-ku, Kitakyushu-city, Fukuoka 808-0196, JAPAN

Correspondence to: Haruo Nishida (E-mail: *nishida@lsse.kyutech.ac.jp*)

((Additional Supporting Information may be found in the online version of this article.))

ABSTRACT

In order to achieve the effective interface bonding between biomass microfiller and commodity plastics, consecutive copolymerization of hydrophilic acrylic acid (AA) and hydrophobic butyl acrylate (BA) using vapor-phase assisted surface polymerization (VASP) technology was applied to prepare micro composites consisting of cellulose micro crystal (CμC) and polypropylene (PP). After the copolymerization by VASP, CμC surfaces were covered by accumulated polymers: P(AA-*co*-BA) including block-type copolymer and homopolymers of 6.2-25.3 wt% versus CμC. Although structures of the products were unspecified, it was expected to be mixtures of block copolymers and homopolymers. Subsequently prepared P(AA-*co*-BA) on CμC/PP (5/95 wt/wt) composites expressed a superior mechanical toughness, which had increased threefold when compared to intact CμC/PP composite. This increase in toughness was mainly based on an increase in elongation rate, reflecting improvement of the adhesion strength at the interface between CμC surface and PP. The trace amounts: 0.31 wt% of accumulated P(AA-*co*-BA) on CμC surface must function as an effective adhesive/compatibilizer at the interface.

INTRODUCTION

If a sustainable society is to be achieved alongside economic development then the world's abundantly available natural resources have a critical role to play. Against this background, the cellulosic materials derived from agricultural and forestry residues have attracted considerable interest from researchers in the field of composite materials.[1] Compared with typical artificial reinforcing fibers such as glass, steel, and carbon fibers, cellulosic materials, as well as being relatively harmless, have some uniquely advantageous properties such as biodegradability, hydrophilicity, high crystallinity, low density, and relatively superior mechanical strength.[2] Reinforcement of plastics by natural fibers is not only a method of producing environmentally benign composites, but also a practical method for preparing excellent high-performance composites, because the natural fibers' mechanical performance compares favorably to steel and glass fibers. For this reason, cellulosic materials, especially cellulose fibers, have been widely used to improve the mechanical properties of polymeric materials.[3,4]

Although various natural fiber reinforced plastic composites have been developed, the natural fibers have not always performed to their potential. One of the main reasons for this limited reinforcement effect has been inadequate adhesion at the interface with plastics. In order to strengthen the adhesion, it is vital that more effective treatments by chemicals and compatibilizers as bonding agents are used between the natural fiber and plastic.[5,6] An ideal compatibilizer has to consist of hydrophilic and hydrophobic segments so as to be compatible with the biomass and plastic, respectively. Other important requirements are that each segment has a high molecular weight sufficient to give adhesive strength to the corresponding component, and that the compatibilizer covers the component surface widely, uniformly, and thinly. In this way a truly effective interface bonding can be achieved.[7]

Vapor-phase assisted surface polymerization (VASP) causes polymer molecules to cover over such things as nano-micro scale gaps and holes in the complex surfaces of a biomass.[8-10] Moreover, VASP shows its living nature in having a proportional relation between number average molecular weight and polymer yield, and in the production of block copolymers by consecutive copolymerization. This copolymerization occurs even in the case of free-radical polymerization, because active species at growing chain ends are immobilized on the substrate surface.[11] These surface modification properties of VASP and its living nature suggest that it is capable of producing effective adhesion at interfaces between biomasses and plastics by being sufficiently compatible. Kim *et al.*[12] prepared composites from wood flour and poly(L-lactic acid) and demonstrated the grafting of polymer chains on wood flour surfaces, which showed a very high crystallinity of 79.2%.

In this study, using VASP technology, hydrophilic and hydrophobic monomers: acrylic acid (AA) and butyl acrylate (BA) having carboxyl and butyl groups, respectively, were selected for showing affinity with both cellulose and matrix polymer, and copolymerizability due to the same acrylic group. The monomers were consecutively copolymerized to obtain surface modified biomass reinforcements that displayed a sufficient adhesive strength at the biomass-plastic interface. Moreover, the mechanical properties of composites that had been prepared from the modified biomass and polypropylene (PP) were evaluated. Taking the melt-processability of composites into account, cellulose micro crystal (CμC) was employed as the biomass due to its good flowability. As a result, trace amounts of accumulated polymers: P(AA-*co*-BA) including block-type copolymer and homopolymers on CμC surface functioned as an effective adhesive/compatibilizer at the interface of CμC and PP, expressing a superior mechanical toughness.

EXPERIMENTAL

Materials

Monomers: acrylic acid (AA, >98.0% by GC) and butyl acrylate (BA, >98.0% by GC) were purchased from Wako Pure Chemical Industries, Ltd. (Wako, Japan), and purified by distillation under reduced pressure. Initiators: azobisisobutyronitrile (AIBN, >98.0% by GC) and benzoyl peroxide (BPO, >98.0% by GC), and inhibitor: 4-tert-butylpyrocatechol were purchased from Wako and Tokyo Chemical Industry Co., Ltd. (TCI, Japan), respectively, and used as received. Cellulose micro crystal (particle size: 3-60 μm) as biomass was obtained from Merck KGaA (Germany). Solvent: dichloromethane (CH_2Cl_2) was obtained

from Wako and used as received. Poly(acrylic acid) (PAA, Mw 450,000) and poly(butyl acrylate) (PBA, Mw 99,000) as references were purchased from Sigma-Aldrich Co. LLC (USA).

Consecutive Copolymerization on CμC Surface by VASP Technology

Consecutive copolymerization of AA and BA as hydrophilic and hydrophobic monomers, respectively, was carried out on initiator-supported CμC (particle size: 3-60 μm) surface in a glass tube reactor (diameter 15 mm × length 14.7 cm) (Figure 1).

In a typical procedure, initiator: AIBN (20 mg, 121.8 μmol) or BPO (20 mg, 82.6 μmol) was dissolved in CH_2Cl_2 (15 mL). The initiator solution was mixed with CμC (5 g), followed by the removal of solvent under reduced pressure for 8 h at room temperature, resulting in the preparation of initiator-supported CμC. VASP was conducted in a monomer vapor fed from an impinger, including a liquid monomer and inhibitor: 4-tert-butylpyrocatechol with N_2 flow (50 mL/min) in an oven (Figure 1). The monomer vapor was constantly evaporated by bubbling N_2 into the impinger. Amounts of the monomer supply were shown in footnote of Table 1. A glass tube reactor was filled up with the initiator-supported CμC (5 g). The glass-tube reactor and impingers were then set in the oven which was thermostated at 70 °C having regard to the 10 h half-life temperatures of 65 and 73.6 °C for AIBN and BPO, respectively. Polymerization time was properly set according to the polymerizability of each monomer. After polymerization, the treated CμC was dried at 70 °C for 8 h under reduced pressure (ca. 0.1 kPa) to remove unreacted monomers adsorbed on the CμC surface, resulting in the preparation of copolymers: P(AA-*co*-BA) on CμC. As references, homopolymerizations of AA and BA were also carried out in the same manner, resulting in the preparation of homopolymers: PAA on CμC and PBA on CμC, respectively.

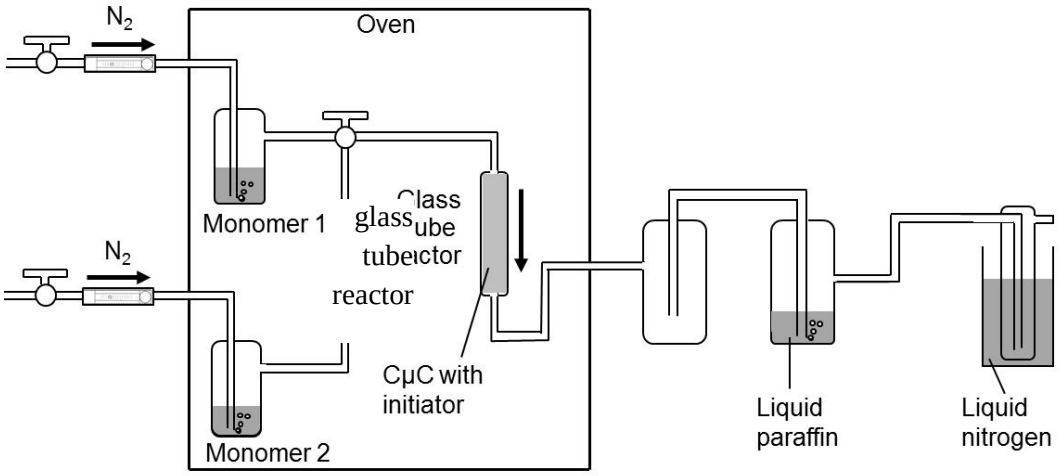

Figure 1. Copolymerization diagram with VASP technology.

Characterization

Accumulated materials on the CμC surface were analyzed with a 3D laser scanning confocal microscope, FTIR, ^{1}H NMR, size exclusion chromatograph, thermogravimeter (TG) and differential TG (DTG).

Morphologies of accumulations on the surface were observed with a 3D laser scanning confocal microscope model VK-X 100/105 (KEYENCE, Japan) under prescribed conditions of laser: red semiconductor laser, λ = 658 nm, 0.95 mW, and pulse width 1 ns.

Chemical structure of the accumulations was analyzed by Fourier transform infrared (FTIR) spectroscopy, which was recorded on a Nicolet iZ10 attached SMART iTR (Thermo Fisher Scientific, Japan) in a wavenumber range of 650-4000 cm^{-1} at a resolution of 4 cm^{-1}. Transmission spectra were measured from a KBr disc coated with polymer samples. Reflection spectra of samples were measured on an attenuated total reflectance (ATR) module with a Zinc selenide crystal, by the single-reflection ATR method. Moreover, microscopic FTIR mapping of the accumulated substrate surface was achieved on a microscopic FTIR equipped with an image-mapping system Nicolet iN10 MX (Thermo Fisher SCIENTIFIC, Japan): in the reflection absorption mode and in a wavenumber range of 675-4000 cm^{-1}.

Absorption intensity of the FTIR spectrum depends on the absorption coefficient specific to each absorption band. In the case of the same absorption band, the intensity increases in proportion to the quantity of the accumulation. Peak area, representing the intensity of each absorption band, was evaluated by peak-fitting software PeakFIT (HULINKS Inc., Japan). The quantity of accumulation was estimated from a calibration curve, which was prepared by measuring FTIR spectra of mixtures with prescribed weight ratios of (PAA + CμC) or (PBA + CμC). Calibration curves of PAA and PBA on CμC were prepared based on specific absorption peaks: $\nu_{C=O}$ derived from carboxyl and ester groups at 1714 and 1735 cm^{-1}, respectively.

The accumulated materials on CμC (100 mg) were dispersed in dimethyl sulfoxide-d_6 (DMSO-d_6 $(CD_3)_2SO$) (2 mL) and filtrated through a cotton filter in a sample tube for ^{1}H NMR measurements. ^{1}H NMR spectra of the dissolved materials were recorded on a 500-MHz JEOL JNM-ECP500 FT NMR system. The chemical shift was reported as δ values (ppm) relative to internal tetramethylsilane (TMS) unless otherwise noted.

The accumulated materials on CμC (100 mg) were dispersed in chloroform (2 mL) and filtrated through a membrane filter with a 0.45 μm pore size for size exclusion chromatograph (SEC) measurements. Molecular weights of the dissolved materials were measured on a TOSOH HLC-8120 SEC apparatus with refractive index (RI) and ultraviolet (UV, λ = 254 nm) detectors under the following conditions: TSKgel Super HM-H linear column (linearity range, 1×10^3 - 8×10^6; molecular weight exclusion limit, 4×10^8), $CHCl_3$ (HPLC grade) eluent at a flow rate of 0.6 $mL \cdot min^{-1}$, and column temperature of 40 ºC. Calibration curves for SEC analysis were obtained using polystyrene standards with polydispersity values lower than 1.10 (weight average molecular weight = 7.70×10^2, 2.43×10^3, 3.68×10^3, 1.32×10^4, 1.87×10^4, 2.93×10^4, 4.40×10^4, 1.14×10^5, 2.12×10^5, 3.82×10^5, 5.61×10^5, 2.00×10^6) (Aldrich).

TG and DTG measurements were conducted on a SEIKO Instruments Inc. EXSTAR 6200 TG system (Japan) in aluminum pans (5 mm in diameter) at a prescribed heating rate, φ, of 9 °C min^{-1} in a temperature range of 50 to 550 °C under a constant nitrogen flow (100 mL min^{-1}) using about 5 mg of sample. A blank aluminum pan was used as a reference. The pyrolysis data were collected at regular intervals (about 20 times $ºC^{-1}$) by an EXSTAR 6000 data platform, and recorded into an analytical computer system.

Melt-Blending with Polypropylene

In order to evaluate the contribution of the accumulated copolymers on CμC to the mechanical properties of composites, P(AA-*co*-BA) on CμC was melt-blended with polypropylene (PP) in a prescribed weight ratio of P(AA-*co*-BA) on CμC:PP = 5:95 (wt/wt). A twin-screw extruder IMC-160B (Imoto Machinery Co., Ltd., Japan, screw diameter 20 mm, L/D 25) equipped with an air vent was used for blending under temperature profiles of 80, 180, 180, and 180°C for four zones from hopper to die with a screw rotational speed of 25 rpm.[13] Extruded strand of P(AA-*co*-BA) on CμC/PP composite was cut into pellets with a pelletizer. Other composite samples: PAA on CμC. PBA on CμC, and neat CμC as references were also melt-blended with PP in the same manner.

Casting sheet samples (10 × 40 mm^2, thickness 0.3 mm) were prepared from the melt-blended composite pellets by heat-pressing with a compact heating press IMC-180C (Imoto Machinery Co., Ltd., Japan) at 180 ºC and 50 MPa for 5 min.

Mechanical Properties of Composites

Mechanical properties of composites were measured by a tensile strength test of specimens (5 × 40 mm^2, thickness 0.3 mm) cut from the casting sheet samples. The tensile strength tests of the composite specimens were conducted on a compact tensile and compression tester IMC-18E0 (Imoto Machinery Co., Ltd., Japan) at a tensile rate of 1 mm·min^{-1}. The tensile test was repeated 20 times and mechanical properties: tensile strength, tensile modulus, and toughness values were calculated from strain-stress curves (S-S curves).

RESULTS AND DISCUSSION

Consecutive Copolymerization on Initiator-Supported CμC Surface

Consecutive copolymerization was carried out for 2 + 2 h (4 h in total) at 70 °C in the order of AA and BA, because hydrophilic PAA segment should first cover the hydrophilic CμC surface, followed by an accumulation of hydrophobic PBA segment. Two initiators AIBN and BPO were employed. AIBN has lower 10-hr half-life temperature and higher initiator efficiency than BPO. On the other hand, BPO has good H-abstraction ability[14] that may be effective for grafting from the cellulose surface. After the copolymerization using AIBN and BPO as initiators, obtained CμC: P(AA-*co*-BA) on CμC increased in weight by 0.1935 and 0.0907 g, resulting in increases of 3.87 and 1.25 wt%, respectively. As references, homopolymerization of AA and BA was carried out under the same conditions (2h at 70 °C) to prepare PAA on CμC and PBA on CμC. In the cases without initiator no polymer was produced on CμC surface.

Figure 2 shows typical SEM images of CμC surface before and after VASP of AA and BA. As result of whole SEM observation, no discernible difference was shown on the CμC surfaces

even under higher magnifications by x 20,000 (Figure S1 in Supporting Information), suggesting a very thin layered coating of copolymers by VASP.

Intact CµC

CµC modified by VASP of AA and BA

Figure 2. SEM images of CµC surface before and after VASP of AA and BA. Bar: 1µm

In order to confirm the accumulation of copolymer, FTIR analysis of P(AA-*co*-BA) on CµC was performed by the transmission method with a KBr disc. In Figure 3, characteristic absorption peaks of P(AA-*co*-BA) on CµC were shown with reference spectra of PAA on CµC, PBA on CµC, and intact CµC. These spectra were normalized based on a characteristic absorption of $\nu_{C=C, \text{aromatic skeletal mode}}$ at 1635 cm^{-1} derived from CµC.[15]

In the spectra, characteristic peaks were detected at 1700-1720 and 1747 cm^{-1} corresponding to the specific absorption bands: $\nu_{C=O}$ of carboxyl and ester groups of PAA on CμC and PBA on CμC. The spectrum of P(AA-*co*-BA) on CμC showed both the absorption bands at 1700-1720 and 1730-1740 cm^{-1}, which were derived from PAA and PBA segments in P(AA-*co*-BA) on CμC. From these results, it was suggested that P(AA-*co*-BA), PAA, and PBA had accumulated on the CμC surface.

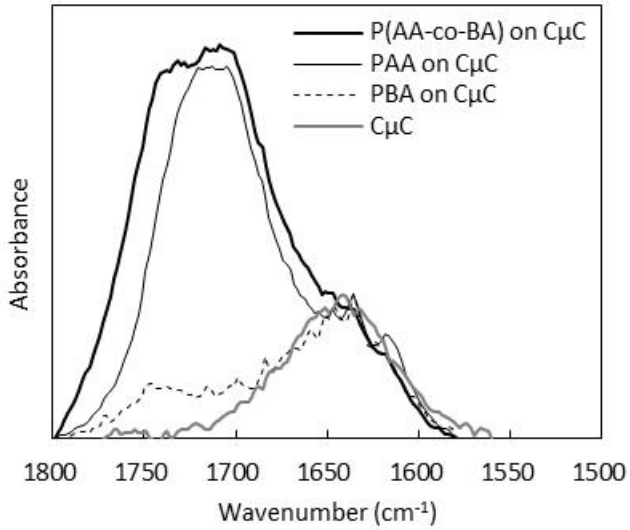

Figure 3. FTIR spectra of copolymer and homopolymers prepared by consecutive copolymerization and homopolymerization using AIBN, respectively, of AA and BA on CμC by VASP technique. These spectra were normalized based on a characteristic absorption of $\nu_{C=C,\text{aromatic skeletal mode}}$ at 1635 cm^{-1} derived from CμC.

The quantity of accumulation was estimated from a calibration curve, which was prepared by measuring FTIR spectra of mixtures with prescribed weight ratios of (PAA + CμC) or (PBA + CμC) (Figure S2). Calibration curves of PAA and PBA on CμC were prepared based on specific absorption peaks: $\nu_{C=O}$ derived from carboxyl and ester groups at 1714 and 1735 cm^{-1}, respectively (Figure S3). Resulting composition ratios of PAA and PBA segments in $P(AA\text{-}co\text{-}BA)_{AIBN}$, $P(AA\text{-}co\text{-}BA)_{BPO}$, PAA_{AIBN}, PAA_{BPO}, PBA_{AIBN}, and PBA_{BPO} accumulated on CμC were listed in Table 1.

From the results in Table 1, it was confirmed that the accumulation contents of $P(AA\text{-}co\text{-}BA)_{AIBN}$ and $P(AA\text{-}co\text{-}BA)_{BPO}$ of 25.3 and 6.2 wt % respectively were higher than the corresponding values of 3.87 and 1.25 wt% calculated from the weight increase,. Segment compositions were found as PAA:PBA = 45.8:54.2 and 64.5:35.5 (wt/wt), respectively, showing different accumulation behaviors depending on both kind and loaded amount of initiator[11]. The homopolymerization of AA and BA indicated a more preferable accumulation of PAA than PBA. These contradictory findings may be induced by various uncontrollable factors, such as chain transfer reactions on the biomass surface and termination reactions which may have a tendency to occur on the CμC surface in the early stages during the induction period.[16]

There may be some explanation for the relatively high P(AA-*co*-BA) accumulation value 25.3 and 6.2 wt% versus CμC compared to 3.87 and 1.25 wt% calculated from the weight increase. One possible reason may be leakage of CμC micro powder during the polymerization in the gaseous flow of 50 mL min^{-1}.

Table 1. Composition ratios of PAA and PBA segments in P(AA-*co*-BA), PAA, and PBA accumulated on CμC.

	PAA (%)	PBA (%)	CμC (%)
$P(AA\text{-}co\text{-}BA)_{AIBN}$ on CμC[a]	11.6	13.7	74.7
PAA_{AIBN} on CμC[a]	12.5	-	87.5
PBA_{AIBN} on CμC[a]	-	2.1	97.9
$P(AA\text{-}co\text{-}BA)_{BPO}$ on CμC[b]	4.0	2.2	93.8
PAA_{BPO} on CμC[b]	2.5	-	97.5
PBA_{BPO} on CμC[b]	-	0.8	99.2

Monomer supply: [a] AA 14.69 mg min^{-1} (0.2039 mmol min^{-1}), BA 17.44 mg min^{-1} (0.1360 mmol min^{-1}); [b] AA 23.91 mg min^{-1} (0.3318 mmol min^{-1}), BA 18.60 mg min^{-1} (0.1451 mmol min^{-1}).

In order to analyze the chemical structures of the accumulated materials with ^{1}H NMR, P(AA-*co*-BA) on CμC, PAA on CμC, and PBA on CμC were agitated in DMSO-d_6 resulting in free accumulated materials being dissolved in the solvent. The solution was filtrated and measured with ^{1}H NMR spectra (Figure 4).

Resonance peaks of butyl group protons of BA unit in P(AA-*co*-BA) on CμC were detected at chemical shift values: δ (ppm) of 0.8-0.9 ($C\underline{H}_3$-CH_2-CH_2-CH_2-), 1.30-1.40 (CH_3-$C\underline{H}_2$-CH_2-CH_2-), 1.60-1.65 (CH_3-CH_2-$C\underline{H}_2$-CH_2-), and 4.10-4.15 (-$C\underline{H}_2$-OCO-) as triplet, multiplet, multiplet, and triplet signals, respectively. Two resonance peaks of protons in the main chain consisting of AA and BA units were detected at δ (ppm) of 1.4-1.5 (-$C\underline{H}_2$-CH<) and 3.0-3.1 (-CH_2-$C\underline{H}$<) as broad peaks.[17]

Accumulated materials dissolved from PAA on CμC and PBA on CμC showed individual ^{1}H NMR spectra. Butyl group protons in PBA were detected at δ (ppm) of 0.8-0.9 ($C\underline{H}_3$-CH_2-CH_2-CH_2-), 1.28-1.34 (CH_3-$C\underline{H}_2$-CH_2-CH_2-), 1.50-1.55 (CH_3-CH_2-$C\underline{H}_2$-CH_2-), and 4.00-4.05 (-$C\underline{H}_2$-OCO-) as triplet, multiplet, multiplet, and double triplet signals, respectively. Protons in the main chain derived from PAA and PBA

were detected at δ (ppm) of 1.4-1.5 (-C<u>*H*</u>$_2$-CH<) and 3.0-3.1 (-CH$_2$-C<u>*H*</u><) as broad peaks similar to those of P(AA-*co*-BA) on CμC.

It is considered that gaps in the chemical shift of protons in butyl groups of P(AA-*co*-BA) and PBA are attributable to a polarity change caused by the coexistence of copolymerized AA units. From the above results, it was determined that AA and BA copolymerized on CμC surface.

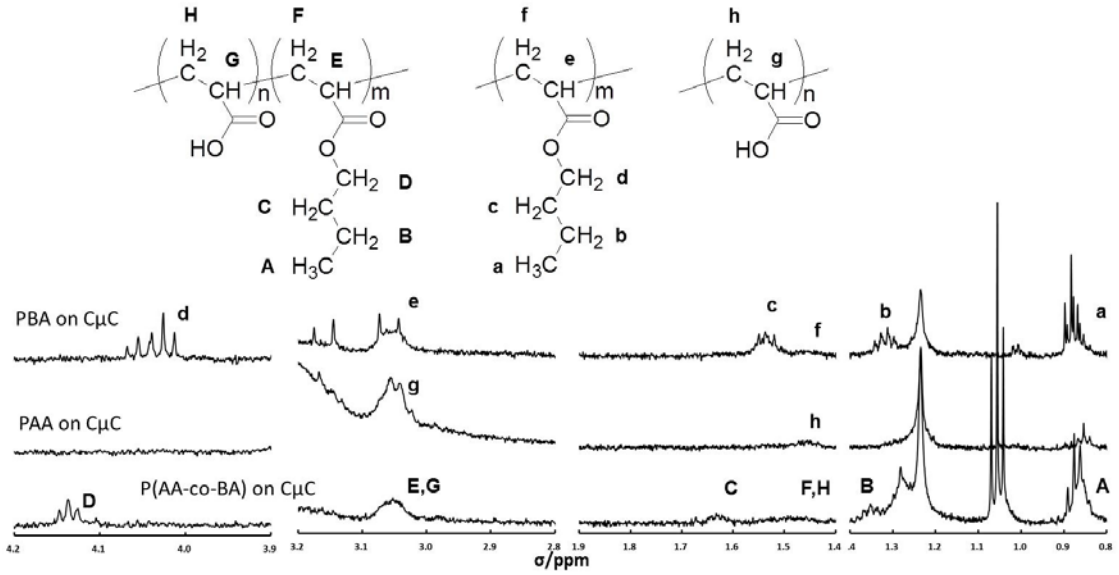

Figure 4. ^{1}H NMR spectra of free accumulated materials dissolved from P(AA-*co*-BA)$_{AIBN}$ on CμC, PAA$_{AIBN}$ on CμC, and PBA$_{AIBN}$ on CμC. Solvent: DMSO-d_6

In order to confirm the molecular weight of copolymers accumulated on CμC, SEC analysis was conducted. P(AA-*co*-BA) on CμC was dispersed in chloroform and stirred to dissolve free accumulated copolymers. The dispersed solution was filtrated and obtained polymer solution was analyzed with SEC using chloroform as eluent. In Figure 5, SEC profiles detected with RI were illustrated, resulting in the confirmation of polymers having single modal profiles and high molecular weights as listed in Table 2. The single modal profiles suggest the copolymer production, not simple blends of homopolymers. The high molecular weight values may be apparent values because of a partial aggregation structure among hydrophilic AA-segments, because P(AA-*co*-BA)$_{BPO}$ on CμC having higher content of AA-unit as listed in Table 1 showed higher molecular weight apparently.

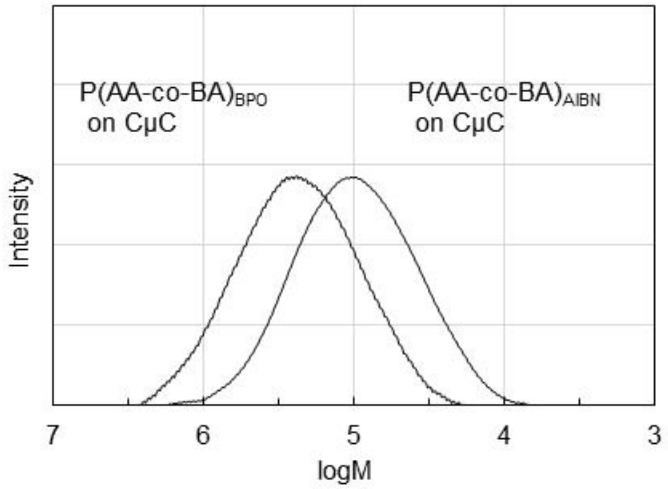

Figure 5. SEC spectrum of free accumulated material dissolved in chloroform from P(AA-*co*-BA) on CμC.

Table 2. Weight average molecular weights (M_w) of free accumulated material dissolved in chloroform from P(AA-*co*-BA) on CμC. Calculated on the basis of polystylene (PSt) standards.

	M_n	M_w
P(AA-*co*-BA)$_{AIBN}$ on CμC	66,000	145,000
P(AA-*co*-BA)$_{BPO}$ on CμC	161,000	346,000

Mechanical Properties of P(AA-*co*-BA)$_{AIBN}$ on CμC/Polypropylene Composites

The accumulated samples: P(AA-*co*-BA) on CμC, PAA on CμC, PBA on CμC, and intact CμC were melt-blended with PP to prepare composite samples by the same weight ratio of modified/neat CμC:PP = 5:95 (wt%), which meant P(AA-*co*-BA)$_{AIBN}$: CμC :PP = 1.27 : 3.73 : 95.00 (wt%) and P(AA-*co*-BA)$_{BPO}$: CμC :PP = 0.31: 4.69 : 95.00 (wt%). Obtained melt-blended composite pellets were heat-pressed to convert them into casting sheet samples (thickness 0.3 mm). The sheet sample of P(AA-*co*-BA) on CμC/PP is shown in Figure S4 with an intact CμC/PP sheet as a reference. Obviously, P(AA-*co*-BA) on the CμC/PP sheet showed a smaller number of agglomerations of modified CμC than the intact CμC/PP sheet, indicating a more homogeneous dispersion of CμC in the PP matrix.

The mechanical properties were measured by a tensile test using specimens prepared from casting sheet samples. In Figure 6, typical strain-stress curves of P(AA-*co*-BA) CμC/PP and intact CμC/PP composites were illustrated. There was no significant difference in tensile strength and modulus values between both the composites resulting from the presence of the small amount (5%) of modified/intact CμC. Significant superiority in toughness was confirmed by 1.7 and 3.0 times values of P(AA-*co*-BA)$_{AIBN}$ on CμC/PP and P(AA-*co*-BA)$_{BPO}$ on CμC/PP composites, respectively, compared to intact CμC/PP

composite (Figure 7). The performance of composite is depended on interfacial affinity and adhesion, which are influenced by some factors: composition of CμC and PP, surface area of CμC, content of copolymers, compositions of AA and BA-units, sequence length of block copolymer, etc. The increase in toughness is mainly based on the increase in elongation rate, reflecting an improvement in the adhesive strength at the interface between CμC and PP. Thus, the trace amounts: 1.265 and 0.31 wt% of accumulated P(AA-*co*-BA)$_{AIBN}$ and P(AA-*co*-BA)$_{BPO}$ on CμC surface, respectively, must function as effective adhesives/compatibilizers at the interface.

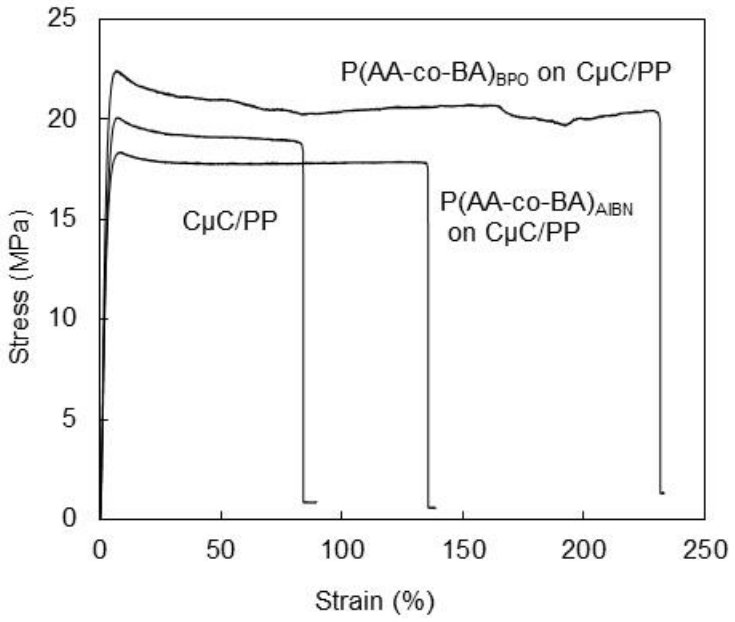

Figure 6. Typical strain-stress curves of P(AA-*co*-BA) on CμC/PP and intact CμC/PP composites.

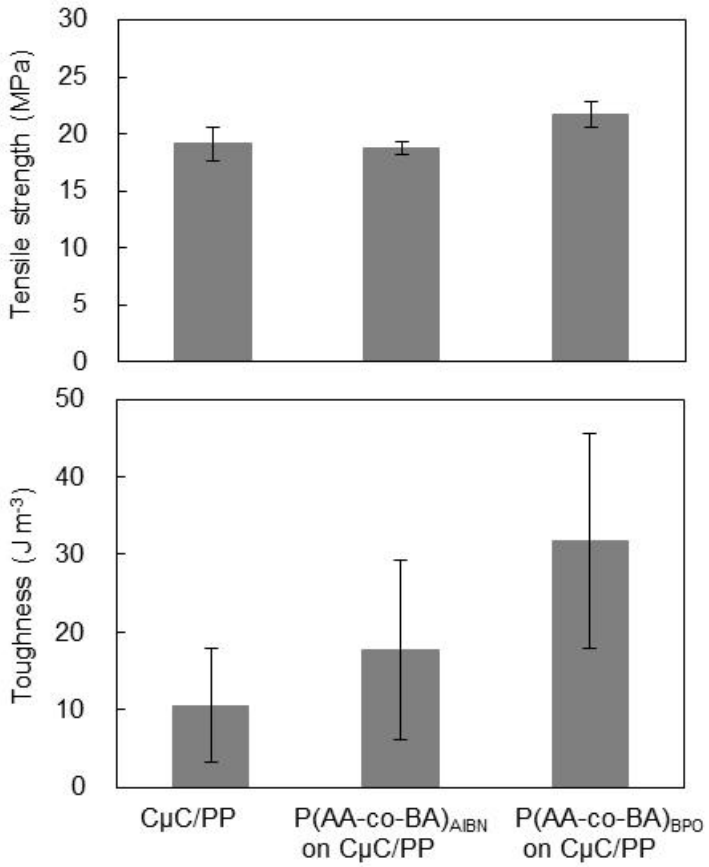

Figure 7. Tensile strength, modulus, and strain energy values of P(AA-*co*-BA) on CμC/PP and intact CμC/PP composites. Bar: standard deviation values.

CONCLUSIONS

In order to achieve the effective interface bonding between CμC and PP, consecutive copolymerization of hydrophilic AA and hydrophobic BA monomers using VASP technology was applied in the preparation of CμC/PP composites. After VASP, the surface of modified CμC was covered by copolymer. Obtained copolymer was characterized as P(AA-*co*-BA) and confirmed to cover the CμC surface as a thin layer. Finally, composites consisting of P(AA-*co*-BA) on CμC and PP (5/95 wt/wt) expressed a threefold superior mechanical toughness compared to intact CμC/PP composite, despite the presence of only a trace amount: 0.31 wt% of accumulated P(AA-*co*-BA) on the CμC surface. The increase in toughness was mainly based on the increase in elongation rate, reflecting improvement of the adhesive strength at the interface between the CμC surface and PP. The improved toughness of composites will be effective for many applications such as parts of housing materials, automobile, and electric appliances in a future.

REFERENCES AND NOTES

1. Thakur, V. K.; Thakur, M. K.; Gupta, R. K. *Int. J. Polym. Anal. Ch.* **2014**, *19*, 256-271.
2. Cruz, J.; Fangueiro, R. *Procedia Engineer.* **2016**, *155*, 285-288.
3. Thakur, V. K.; Thakur, M. K.; *Carbohyd. Polym.* **2014**, *109*, 102–117.
4. Asokan, P.; Firdoous, M.; Sonal, W. *Rev. Adv. Mater. Sci.* **2012**, *30*, 254-261.
5. Herrera-Franco, P. J.; Valadez-Gonza´lez, A. *Compos. Part B-Eng.* **2005**, *36*, 597–608.
6. Li, X.; Tabil, L. G.; Panigrahi, S. *J. Polym. Environ.* **2007**, *15*, 25–33.
7. Wang, Y.; Chen, F.-B.; Wu, K.-C.; Wang, J.-C. *Polym. Eng. Sci.* **2006**, *46*, 289-302.
8. Nishida, H.; Andou, Y.; Endo, T. In In Situ Synthesis of Polymer Nanocomposites; Mittal, V., Ed.; Wiley-VCH: Germany, **2011**; Chapter 4, pp. 89-104.
9. Andou, Y.; Jeong, J.-M.; Kaneko, M.; Nishida, H.; Endo, T. *Polym. J.* **2010**, *42*, 519-524.
10. Lee, H.-S.; Wakisaka, M.; Nagasawa, N.; Nishida, H.; Andou, Y. *Kobunshi Ronbunshu* **2014**, *71*, 31-37
11. Yasutake, M.; Hiki, S.; Andou, Y.; Nishida, H.; Endo, T. *Macromolecules* **2003**, *36*, 5974-5981.
12. Kim, D.; Andou, Y.; Shirai, Y.; Nishida, H. *Appl. Mater. Interfaces* **2011**, *3*, 385–391.
13. Yamashiro, K.; Nishida, H. *Int. J. Biomass Renewable* **2015**, *4*, 8-16.
14. Lazár, M.; Hrčková, L.; Fiedlerová, A.; Borsig, E. *Macromol. Mater. Eng.* **2000**, *283*, 88-92.
15. Yang, H.; Yan, R.; Chen, H.; Lee, D.-H.; Zheng, C. *Fuel* **2007**, *86*, 1781-1788.
16. Andou, Y.; Yasutake, M.; Jeong, J.-M.; Nishida, H.; Endo, T. *Macromol. Chem. Phys.* **2005**, *206*, 1778-1783.
17. Ahmadian-Alam, L.; Haddadi-Asl, V.; Roghani-Mamaqani, H.; Hatami, L.; Salami-Kalajahi, M. *J. Polym. Res.* **2012**, *19*:9773.

GRAPHICAL ABSTRACT